

# High-Speed Solar Wind Streams and Geomagnetic Storms During Solar Cycle 24

M. Gerontidou<sup>1</sup> · H. Mavromichalaki<sup>1</sup>  · T. Daglis<sup>1</sup>

Received: 24 April 2018 / Accepted: 22 August 2018  
© Springer Nature B.V. 2018

**Abstract** An updated catalog is created of 303 well-defined high-speed solar wind streams that occurred in the time period 2009–2016. These streams are identified from solar and interplanetary measurements obtained from the OMNIWeb database as well as from the *Solar and Heliospheric Observatory* (SOHO) database. This time interval covers the deep minimum observed between the last two Solar Cycles 23 and 24, as well as the ascending, the maximum, and part of the descending phases of the current Solar Cycle 24. The main properties of solar-wind high-speed streams, such as their maximum velocity, their duration, and their possible sources are analyzed in detail. We discuss the relative importance of all those parameters of high-speed solar wind streams and especially of their sources in terms of the different phases of the current cycle. We carry out a comparison between the characteristic parameters of high-speed solar wind streams in the present solar cycle with those of previous solar cycles to understand the dependence of their long-term variation on the cycle phase. Moreover, the present study investigates the varied phenomenology related to the magnetic interactions between these streams and the Earth's magnetosphere. These interactions can initiate geomagnetic disturbances resulting in geomagnetic storms at Earth that may have impact on technology and endanger human activity and health.

**Keywords** High-speed solar wind streams · Coronal holes · Coronal mass ejections · Geomagnetic storms

## 1. Introduction

As is well known, the continuous stream of plasma ejected by the Sun, flowing outward from the corona into and through the interplanetary space with a mean speed of about

---

**Electronic supplementary material** The online version of this article (<https://doi.org/10.1007/s11207-018-1348-8>) contains supplementary material, which is available to authorized users.

---

✉ H. Mavromichalaki  
[emavromi@phys.uoa.gr](mailto:emavromi@phys.uoa.gr)

<sup>1</sup> Nuclear and Particle Physics Department, Faculty of Physics, National and Kapodistrian University of Athens, Zografos, 15784 Athens, Greece

250–400 km s<sup>-1</sup> (Parker, 1959), is called the solar wind. This uninterrupted outflow of plasma frequently contains fast streams, as is obvious from solar plasma space borne observations, known as high-speed solar wind streams (HSSWSs). A more accurate definition of HSSWSs is given by Bame *et al.* (1976) and Gosling *et al.* (1976), who consider as a HSSWS a detected fluctuation of the solar-wind speed increasing by at least 150 km s<sup>-1</sup> within a time interval of five days. In more recent works (Mavromichalaki and Vassilaki, 1998; Xystouris, Sigala, and Mavromichalaki, 2014) an HSSWS is defined as an increase of the solar-wind speed between the highest and the mean plasma speed foregoing and following the stream greater than 100 km s<sup>-1</sup> which lasts at least two days. This definition is also adopted in this study, since the aim of the present work is to update and continue previous ones.

Most previous articles consider HSSWSs to be associated with solar flares (SFs) and coronal holes (CHs) (*e.g.* Lindblad and Lundstedt, 1981, 1983; Lindblad, Lundstedt, and Larsson, 1989; Mavromichalaki, Vassilaki, and Marmatsouri, 1988; Mavromichalaki and Vassilaki, 1998; Xystouris, Sigala, and Mavromichalaki, 2014). After the advent of coronagraphs and the availability of their good quality data, coronal mass ejections (CMEs) instead of solar flares started to have central importance in producing major events in the near-Earth space environment (Cane, 2000; Crooker *et al.*, 2000; Gopalswamy, Yashiro, and Akiyama, 2007; Badruddin and Singh, 2009). Moreover, space-based near-Earth observations of the solar-wind plasma can be distinguished into two types, those related with CMEs and those coming from coronal holes (CHs). As a consequence, there are two classes of interplanetary structures related to these two types of observations, *i.e.* interplanetary coronal mass ejections (ICMEs) originating from closed field regions and corotating interaction regions (CIRs) from open field regions (Gosling *et al.*, 1976; Gopalswamy, Yashiro, and Akiyama, 2007; Jian *et al.*, 2006; Paouris and Mavromichalaki, 2017). Both ICMEs and CIRs are capable of driving shocks in the interplanetary space by interaction between high-speed CMEs and/or CH streams and the ambient solar wind (Gosling *et al.*, 1976; Sabbah, 2000; Jian *et al.*, 2006; Kane, 2007). Adopting this separation, we classify HSSWSs in the solar wind in two types: those coming from solar active regions during CMEs and those coming from diverging and unipolar field regions called CHs.

The basic physical features of CME-generated streams are similar to those referred to as flare-generated streams in the previous work by Xystouris, Sigala, and Mavromichalaki (2014). This means that the CME-generated streams show in all the interplanetary parameters, such as the bulk speed ( $V$ ), the proton density ( $n$ ), and the magnetic field strength ( $B$ ), large fluctuations during the highest speed period indicating fast shocks that are emitted radially, field polarity inversions lasting 3–4 h, and proton temperature not varying simultaneously with the flow speed.

On the other hand, CH-generated streams are less fluctuating than CME-generated streams; the magnetic field strength ( $B$ ) changes with the change of the velocity of the solar wind, the polarity of the magnetic field remains the same during the solar-wind stream, and the proton density ( $n$ ) and temperature ( $T$ ) vary inversely.

Moreover, solar-wind streams with high speed (> 400 km s<sup>-1</sup>) are often observed not only in the near-Earth space, but also in the interplanetary space using space-based data. These high speed streams and their associated structures influence geomagnetic activity (Mavromichalaki, Vassilaki, and Marmatsouri, 1988; Kudela and Brenkus, 2004; Gupta and Badruddin, 2009; Yermolaev *et al.*, 2014; Badruddin and Falak, 2016) and modify space weather conditions (Bothmer and Zhukov, 2007; Badruddin and Kumar, 2015). Some of the previous studies focus on the analysis of the solar sources of HSSWSs and their geoeffectiveness. HSSWSs can be the result of streams from a single coronal hole,

multiple coronal holes, single CME, multiple CMEs, or of a combination of streams from coronal holes and CMEs (Gupta and Badruddin, 2010; Kumar and Badruddin, 2014). In this article we also study how HSSWSs from different sources influence geomagnetic activity, *i.e.* affect the intensity of the resulting geomagnetic storms (Lakhina and Tsurutani, 2016; Aslam and Badruddin, 2017).

We focus our analysis on well-defined high-speed solar wind streams during the period 2009–2016, covering the deep minimum (DeepMin) between Solar Cycles 23 and 24 (SC23 and SC24), the ascending (minimum to maximum, MinMax) and the descending phases of SC24. We catalog the HSSWSs of this period and determine their possible sources, their characteristic parameters, such as their maximum velocity, their beginning and end times, and their duration. Moreover, we analyze the association of the solar sources of these HSSWSs with the occurrence and the intensity of geomagnetic storms. For comparison, we also discuss the behavior of all these parameters during the different phases of SC23.

## 2. Data Selection

We have used the same identification and calculation criteria of high-speed solar wind streams as in Mavromichalaki and Vassilaki (1998) and Xystouris, Sigala, and Mavromichalaki (2014). We consider these criteria to more precisely determine the start and the end times of an HSSWS. The data were obtained from the database in the website Operating Missions as Nodes on the Internet (OMNIWeb) (<http://omniweb.gsfc.nasa.gov/>) and the dates were transformed into Julian dates (JUD) to have a consistent way to process the data using a program in Origin. The following parameters for the period from 1 January 2009 till 31 December 2016 were taken into account: the Bartels rotation number, the solar wind flow speed, proton temperature, magnetic field strength, and proton density. The polarity of the interplanetary magnetic field (IMF) and the changes during the HSSWS and the Bartels rotation were derived from the information in the website [http://omniweb.gsfc.nasa.gov/html/polarity/polarity\\_tab.html](http://omniweb.gsfc.nasa.gov/html/polarity/polarity_tab.html) for all the defined HSSWSs. The scales of the geomagnetic storms associated with the corresponding HSSWSs were taken from the NOAA Space Weather Prediction Center ([http://www.swpc.noaa.gov/NOAA\\_scales](http://www.swpc.noaa.gov/NOAA_scales)).

To identify the possible source of each HSSWS, data obtained from the websites [http://www.solen.info/solar/coronal\\_holes.html](http://www.solen.info/solar/coronal_holes.html) for the CHs and [http://cdaw.gsfc.nasa.gov/CME\\_list/](http://cdaw.gsfc.nasa.gov/CME_list/) for the CMEs were used. As a first step, we started to look for a CME and/or CH two days before the start time of an HSSWS. In the simple case that the source could be clearly distinguished, the criteria were based on the occurrence of a CH or a CME in this time window. But this was not always the case! During more active periods when CMEs followed one after the other and a long-lived CH was also present, the selection of the source was much more complicated. In the cases when more than one source seemed to exist, we tried to identify the main one. If the CME was recorded as a poor event, we considered the CH as the main source. In even more complicated cases, we analyzed the variation of the proton density and magnetic field and tried to find the origin of the HSSWS according to the characteristic features of CHs and CMEs.

Moreover, a classification of the HSSWSs according to their structure into simple (S), multi-peak (M), and interrupted (I) was also done. Adopting again the criteria used in Xystouris, Sigala, and Mavromichalaki (2014), the HSSWSs were classified into the following categories:

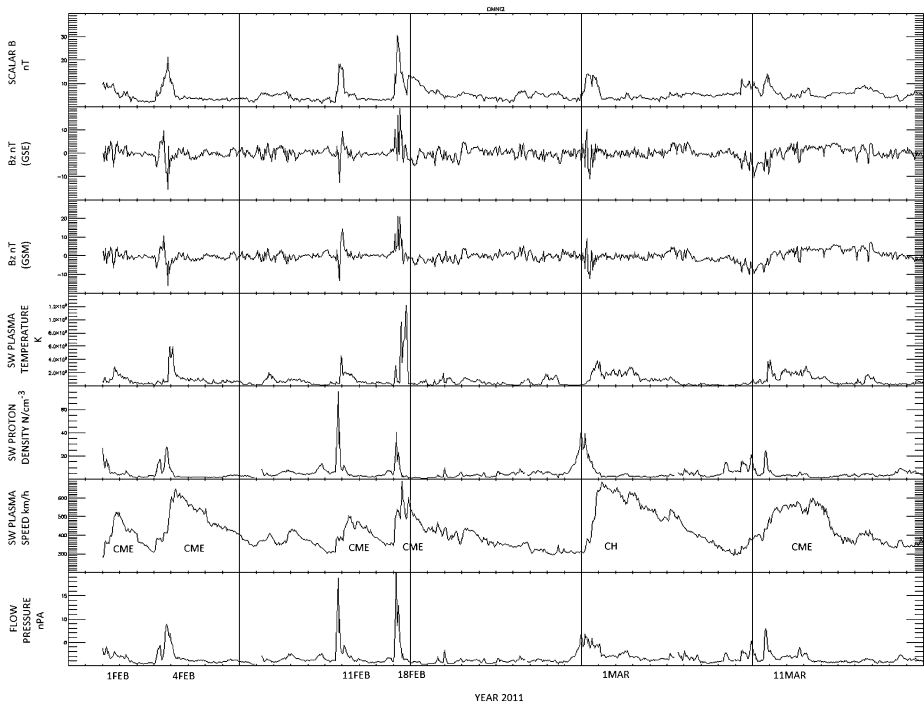


**Figure 1** A typical example of HSSWSs during the period 1 February 2011 till 15 March 2011. Time profiles of the interplanetary parameters  $B$ ,  $B_z$ ,  $T$ ,  $n$ , solar wind speed, and flow pressure show the behavior of HSSWSs associated to CMEs and CHs.

- Simple HSSWSs (S). These have only one peak without any other HSSWSs present for at least 3 h before the start and after the end of the HSSWS.
- Multiple-peak HSSWSs (M). These have more than one peak and every peak is closer to the following one by less than one day.
- Interrupted HSSWSs (I). These present an interruption by another HSSWS that is considered as new and under way. According to this definition, two different phases are distinguished, the rising and the declining ones. The rising phase is determined by the period between the start of the HSSWS and the moment of the maximum velocity. While the declining phase is determined as the period between the time when the HSSWS reaches its highest velocity and its end. Consequently, the interruption may occur either in the rising phase or in the declining one.

Note that in the examined period there were no data gaps and no consecutive HSSWSs were observed.

Typical examples of HSSWSs caused by CMEs or CHs during the period from 1 February 2011 to 15 March 2011 are shown in Figure 1. Time profiles of the interplanetary parameters: magnetic field ( $B$ ),  $z$  component of the magnetic field in GSE coordinates ( $B_z$ ), temperature ( $T$ ), proton density ( $n$ ), solar wind speed, and flow pressure are presented in this figure showing the behavior of HSSWSs associated to CMEs and CHs. Analogous figures were studied for the whole examined period 2009–2016 and all the HSSWSs and their characteristics were identified.

**Table 1** Yearly number of the different categories of HSSWSs during 2009–2016.

| Years | Total number (T) | Simple (S) | Multiple (M) | Interrupted (I) |
|-------|------------------|------------|--------------|-----------------|
| 2009  | 32               | 17         | 13           | 2               |
| 2010  | 38               | 18         | 18           | 2               |
| 2011  | 42               | 19         | 21           | 2               |
| 2012  | 41               | 23         | 14           | 4               |
| 2013  | 39               | 24         | 12           | 3               |
| 2014  | 27               | 17         | 8            | 2               |
| 2015  | 46               | 12         | 29           | 5               |
| 2016  | 38               | 13         | 18           | 7               |
| Total | 303              | 143        | 133          | 27              |

According to the above criteria a number of 303 HSSWSs were identified and a complete catalog, including the interplanetary magnetic field (IMF) polarity and other characteristics, accompanies this article as online supplementary material in the form of a table. The serial number of an is given in the first column of this table, while its date HSSWS appears in the second one. The information of the Bartels rotation (number and day) and the polarity of the IMF for the duration of the HSSWS are given in the third and fourth columns, respectively. The date when the solar wind stream reached its maximum speed is presented in the fifth column. The mean and the maximum values of the solar wind speed are given in columns six and seven, respectively. Finally, the time duration of the HSSWS, its type according to its classification, S for simple HSSWSs, M for HSSWSs having multiple peaks, I for interrupted, and their associated source, symbolized as CH and CME, are shown in columns eight, nine, and ten, respectively. The last column gives the existence or not and the type of associated geomagnetic storms according to the NOAA classification.

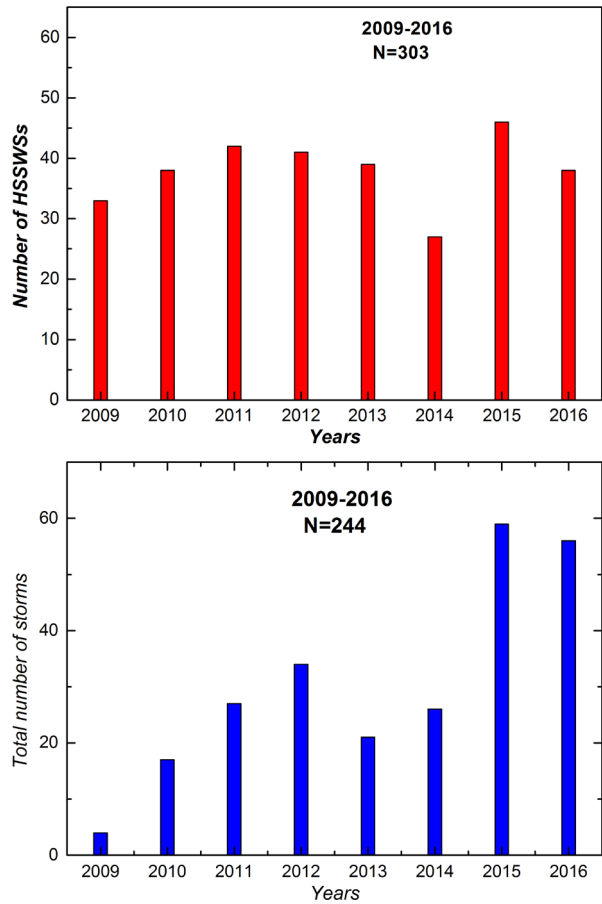
We believe that this catalog can be a useful tool for studies of various solar–interplanetary and solar–terrestrial phenomena and it will complete the study of the HSSWSs starting from Solar Cycle 20 going till the current Cycle 24 (Lindblad and Lundstedt, 1981, 1983; Lindblad, Lundstedt, and Larsson, 1989; Mavromichalaki, Vassilaki, and Marmatsouri, 1988; Mavromichalaki and Vassilaki, 1998; Xystouris, Sigala, and Mavromichalaki, 2014).

### 3. HSSWS Properties

#### 3.1. Occurrence Number

The annual distribution of the HSSWSs is shown in Table 1. The yearly number of the different categories of the streams, simple (S), multiple (M), and interrupted (I), are given in the second, third, and fourth columns of this table, respectively. In 2009 that is at the minimum between the previous solar cycle (SC23) and the parent one (SC24), a percentage of almost 11% of HSSWSs had occurred, while in 2010 a slight increase of 12.5% was registered. In 2011, which is close to the first maximum, and in 2012, which is the first maximum of SC24, a persistent percentage of about 14% occurred, while in 2013 it was 12.8%. In 2014, which is the second maximum of SC24, an unexpected sharp decrease at almost 9% appears. A possible explanation can be given based on the heliographic location of the coronal holes. According to de Toma (2011) at the beginning of 2009 the majority

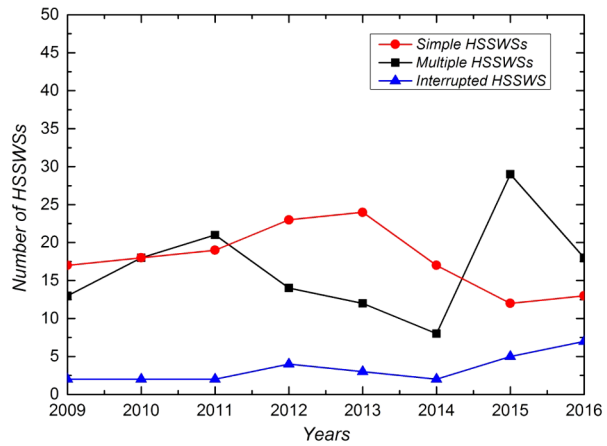
**Figure 2** Yearly distribution of the total number of the HSSWSs (*upper panel*) and the corresponding number of geomagnetic storms (*lower panel*) for the time interval 2009–2016.



of coronal holes located at low-latitude regions had closed down almost simultaneously, with the increase of the solar activity of the new SC24, small coronal holes situated at mid-latitude regions appeared. Note that these small coronal holes were quiet and quickly changing transients (Wang, 2010) and their combined area extended over less than 1.5% of the Sun's surface. These smaller and brief-lived CHs were not considered to be significant sources of solar wind plasma reaching Earth. So, the new configuration of coronal holes shifted the sources of the solar wind reaching Earth to higher latitudes, with the solar wind coming principally from the edges of the polar coronal holes and occasionally from the small mid-latitude coronal holes. In 2015 and 2016, as we were going to the minimum of this cycle, values of 15% and 12%, respectively, occurred. The yearly number of the HSSWSs during the examined time interval is presented in the upper panel of Figure 2. The 11-year distribution during the current solar cycle is obvious, although in 2015 and 2016, close to the end of this cycle, the number of HSSWSs increased significantly. We note that during these years also the number of the geomagnetic storms occurring at Earth increased as shown in the bottom panel of Figure 2 (Aslam and Badruddin, 2017).

It is important to mention that the number of HSSWSs within the time spanning the rising phase of SC24 was smaller than that of SC23. According to Xystouris, Sigala, and Mavromichalaki (2014), the number of HSSWSs during the rising phase of SC23 was about

**Figure 3** Time distribution of the total number of the three types of HSSWSs, simple, multiple, and interrupted, for the time period 2009–2016.



6 HSSWSs *per month*, while at the rising phase of SC24 it was approximately 3 HSSWSs *per month*. A large percentage of 35% of the total number of HSSWSs occurring in the current solar cycle is observed during the maximum phase, while there is no big difference between the percentages of the rising and declining phases, which are 27% and 26%, respectively. Note that at the minimum of SC24 there are fewer HSSWSs with a percentage of 23% of the total number. These results are in agreement with the corresponding ones concerning the previous solar cycles (20, 21, and 22). Maris and Maris (2005) have shown that the occurrence rate of streams for Solar Cycles 20–22 was higher during the rising and declining phases, independently of their solar sources (coronal holes or solar flares). During 2003 a significant increase of the number of HSSWSs throughout SC23 is observed, reaching approximately six HSSWSs *per month*. During 2003 a great number of extreme solar events, such as those of October–November 2003 (Eroshenko *et al.*, 2004; Belov *et al.*, 2005), took place. Moreover, the year 2005 of the same cycle was characterized by events of strong cosmic ray intensity with peculiar properties (Papaioannou *et al.*, 2009a, 2009b)

It is important to note that during the declining phase of SC24, 2015 presented an analog behavior to 2005 of SC23, characterized by an unexpected intense solar activity with a great number of HSSWSs and geomagnetic effects, the so-called year of geomagnetic storms (Paouris, Gerontidou, and Mavromichalaki, 2016). As seen in Figure 2, the number of the HSSWSs in the ascending and maximum phases of the present solar cycle is more than twice the number in the descending phase.

Concerning the categories of HSSWSs during the examined period shown in Table 1, a sharp increase of the number of multiple HSSWSs is observed during 2015 and 2016, which is analogous to the observed increase of the geomagnetic storms during these years. The yearly number of the HSSWSs according to the categories simple (S), multiple (M), and interrupted (I) is presented in Figure 3.

### 3.2. Duration of HSSWSs

We classify the observed HSSWSs in five different categories according to their duration. The short-lasting HSSWSs have a duration of less than two days, indicated as  $< 2$  days; then we have those between two and four days, four and six days, six and eight days, and eight and ten days. Finally, the long-lasting HSSWSs have durations of ten days or longer and are indicated as  $\geq 10$  days.

**Table 2** Yearly distribution of HSSWS durations during 2009–2016.

| Years        | Duration in days |     |     |     |      |      |
|--------------|------------------|-----|-----|-----|------|------|
|              | < 2              | 2–4 | 4–6 | 6–8 | 8–10 | > 10 |
| 2009         | 0                | 6   | 13  | 9   | 2    | 2    |
| 2010         | 0                | 12  | 11  | 8   | 5    | 2    |
| 2011         | 1                | 16  | 11  | 9   | 4    | 1    |
| 2012         | 0                | 14  | 11  | 6   | 5    | 5    |
| 2013         | 0                | 6   | 17  | 9   | 4    | 3    |
| 2014         | 0                | 7   | 9   | 3   | 5    | 3    |
| 2015         | 1                | 10  | 12  | 8   | 6    | 9    |
| 2016         | 0                | 3   | 11  | 7   | 7    | 10   |
| <i>Total</i> | 2                | 74  | 95  | 59  | 38   | 35   |

**Table 3** Yearly distribution of HSSWS speeds during 2009–2016.

| Years        | Number of HSSWS according to their speed in $\text{km s}^{-1}$ |         |         |         |         |         |
|--------------|--|---------|---------|---------|---------|---------|
|              | 400–499  | 500–599 | 600–699 | 700–799 | 800–899 | 900–999 |
| 2009         | 19   | 12      | 2       | 0       | 0       | 0       |
| 2010         | 17   | 11      | 8       | 1       | 1       | 0       |
| 2011         | 7  | 20      | 10      | 5       | 0       | 0       |
| 2012         | 12   | 17      | 7       | 5       | 0       | 0       |
| 2013         | 11   | 16      | 7       | 4       | 0       | 0       |
| 2014         | 10   | 7       | 5       | 2       | 0       | 3       |
| 2015         | 13   | 16      | 11      | 5       | 1       | 0       |
| 2016         | 6  | 13      | 11      | 8       | 0       | 0       |
| <i>Total</i> | 95   | 112     | 61      | 30      | 2       | 3       |

The annual number of the HSSWs in each of the above speed bins for the time period 2009–2016 is given in Table 3 and is presented in Figure 4. The above separation shows that the dominant HSSWs are those with a duration ranging between four and six days with a percentage of 31.3% out of 303 observed HSSWs. The HSSWs having duration between two–four days and six–eight days with percentages of 24.4% and 19.4%, respectively, follow. The shortest-lasting HSSWs, symbolized as < 2 days and the long-lasting ones, symbolized as  $\geq 10$  days, constitute only 0.6% and 11.5% out of the total 303 HSSWs, respectively. Taking into consideration the statistical errors for each duration bin, the majority of the HSSWs in Solar Cycle 24 lasted from four to six days (Table 2). This conclusion is in agreement with the previous study of Xystouris, Sigala, and Mavromichalaki (2014), as well as with Gupta and Badruddin (2010), where the prevalent HSSWs are the medium-duration high-speed streams with a duration of 4 days  $< t \leq 8$  days (46%).

As we deduce from Figure 3, the distribution of the HSSWS durations in the different phases of the SC24 shows a prominent maximum in duration four–six days during the ascending and descending phases of this solar cycle. This trend seems to be valid also in the second maximum of the solar cycle, while in the first maximum the situation is the opposite, where the HSSWs lasting between two and four days have a pronounced maximum. In



**Figure 4** Yearly distribution of HSSWS durations within the five bins for the time period 2009–2016.

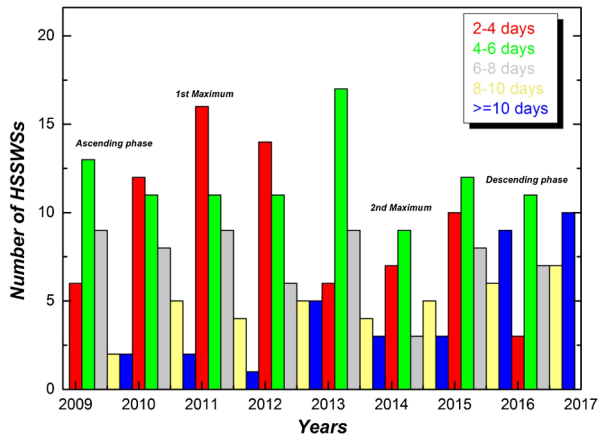
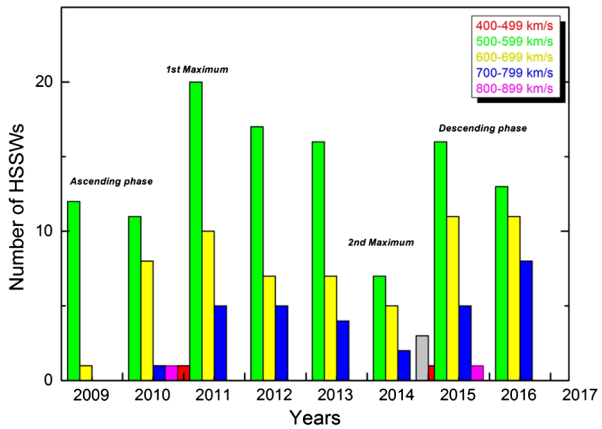


**Figure 5** Yearly distribution of HSSWSs speeds for each of the five bins. The different phases of Solar Cycle 24 are indicated.



comparison with the previous SC23 the majority of the HSSWSs (duration between two–eight days) were more equally distributed in the ascending and descending phases, presenting a slight maximum during the rising phase when compared to the current cycle (Xystouris, Sigala, and Mavromichalaki, 2014).

### 3.3. Maximum Speed

One of the main characteristics of HSSWSs in this catalog is their maximum speed. To analyze their distribution during the whole Solar Cycle 24 and during its different phases, we divided the observed 303 HSSWSs into bins of  $100 \text{ km s}^{-1}$ , from  $400 \text{ km s}^{-1}$  to  $899 \text{ km s}^{-1}$ . It is important to note that there were no data gaps and the results are presented in Table 3. The yearly distribution of HSSWSs according to their maximum speed is presented in Figure 5.

As can be seen, the majority of HSSWSs in a percentage of almost 70% have speeds between  $400\text{--}599 \text{ km s}^{-1}$ . Specifically, a clearly pronounced maximum with a speed between  $500\text{--}599 \text{ km s}^{-1}$  appears during the maximum and declining phases of SC24, constituting a percentage of 37%. Then HSSWSs having a maximum speed in the range  $400\text{--}499 \text{ km s}^{-1}$  follow with a percentage of 31%, while fast HSSWSs with a speed  $700\text{--}799 \text{ km s}^{-1}$  are

**Table 4** Annual number of HSSWSs generated by coronal holes and CMEs for SC24.

| Years        | Total | HSSWS <sub>CH</sub> | HSSWS <sub>CME</sub> |
|--------------|-------|---------------------|----------------------|
| 2009         | 32    | 9                   | 23                   |
| 2010         | 38    | 11                  | 27                   |
| 2011         | 42    | 17                  | 25                   |
| 2012         | 41    | 19                  | 22                   |
| 2013         | 39    | 19                  | 20                   |
| 2014         | 27    | 9                   | 18                   |
| 2015         | 46    | 12                  | 34                   |
| 2016         | 41    | 17                  | 21                   |
| <i>Total</i> | 303   | 113                 | 190                  |

only 0.1% of the total number. It is interesting to note that the fastest HSSWSs with speeds between  $900\text{--}999\text{ km s}^{-1}$  are only 3 out of the total 303 and are observed in the descending phase of the current solar cycle, in particular during 2015.

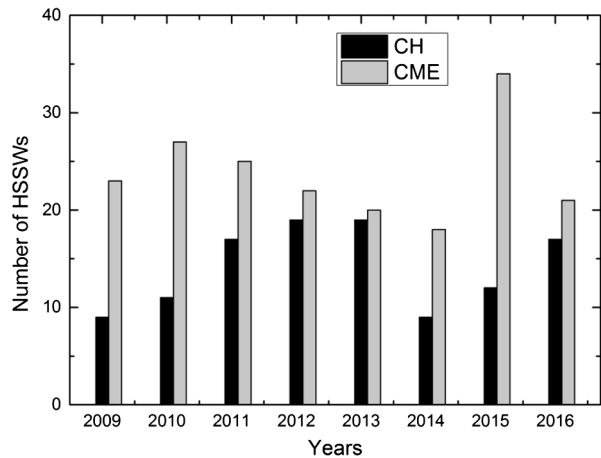
In comparison with the ascending phase of the previous SC23 (Xystouris, Sigala, and Mavromichalaki, 2014) when a great number of HSSWSs had  $V_{\max}$  in the range  $400\text{--}499\text{ km s}^{-1}$ , followed by those within the  $500\text{--}599\text{ km s}^{-1}$  bin and the  $600\text{--}699\text{ km s}^{-1}$  bin, we can say that the same distribution is also observed in the current SC24, while the situation during the descending phase of SC24 is inverse to that of SC23. This means that the number of HSSWSs belonging to the  $500\text{--}599\text{ km s}^{-1}$  bin is bigger than the number of HSSWSs belonging to the  $600\text{--}699\text{ km s}^{-1}$  bin.

### 3.4. Possible Sources

The search of high-speed solar wind stream sources constitutes a key point of the solar-terrestrial and heliospheric physics. As is well known, high-speed streams originate from plasma having high solar wind speed values from coronal holes. The slower solar-wind streams are tightly wound in the Parker spiral in comparison to the HSSWSs at various distances, where the faster solar wind covers the slower wind in front of it. On the other hand, solar-terrestrial effects caused by interplanetary structures and streams originating from CMEs or ICMEs and CHs have been a subject of interest and extensive study. In this sense, it is important to classify the HSSWSs according to their different solar sources. Thus, in the present work, we consider as possible sources of HSSWSs two distinct types of magnetic field structures in the Sun: CMEs and CHs. Therefore, the total number of the defined HSSWSs of the current solar cycle is divided into two groups: a) CME-generated streams and b) corotating streams originated by CHs. Table 4 shows the results of this grouping. It is important to note that an essential difference between this study and previous ones (Xystouris, Sigala, and Mavromichalaki, 2014; Mavromichalaki and Vassilaki, 1998) is the replacement of solar flares as a source of HSSWSs with CMEs, examining simultaneously their possible associated solar flares. This is due to the fact that the advent of coronagraph and space-based near-Earth observations of the solar wind plasma gives the possibility to recognize the HSSWSs as those ejected from solar active regions during CMEs and those coming from coronal holes (Sabbah, 2000; Jian *et al.*, 2006; Kane, 2007).

The yearly distribution of HSSWSs with their different sources is illustrated in Figure 6. We conclude that the majority of HSSWSs are CME-generated streams with a percentage of almost 63%, while corotating streams originating from coronal holes are the remaining

**Figure 6** Yearly distribution of the HSSWS associated sources, CHs and CMEs for the time period 2009–2016.



37%. Note that, although the finding of the possible source of each HSSWS was often complicated, in our study there are no streams with no clear origin. As can be seen from the Figure 6, a great number of CME-generated streams took place during 2015.

### 3.5. HSSWSs in Different Phases of SC23 and SC24

The present SC24 presents in general a smaller amplitude than that of the previous SC23. However, during the rising phases of both SC23 and 24 the number of CMEs is almost the same and even slightly larger in SC23 than in SC24 (Gopalswamy *et al.*, 2014). The examined time period from January 2009 till December 2016 covering SC24 is divided in three different phases, according to the solar activity level:

- The interval from January 2009 to August 2011 is the ascending phase, including the DeepMin between SC23 and SC24.
- The interval from September 2011 to May 2014 is the maximum phase, including the first maximum in 2012 and the second one in 2014 known as MinMax.
- The interval from June 2014 to December 2016 is the descending phase.

In addition, on average the ratio of the number of large sunspot groups in relation to the number of small sunspot groups is larger in the rising phase of SC24 than that in the corresponding phase of SC23, as can be inferred from the Solar Optical Observing Network (SOON) and the Debrecen Photoheliographic Data (DPD) of sunspot group. This could be an indication for the possible reason of the discrepancy in the CME occurrence during the rising phases of SC23 and 24. These results are well connected with the solar cycle mechanism (Kumar and Badruddin, 2014; Badruddin and Falak, 2016).

As a first remark in the present solar cycle the number of HSSWSs is more than twice in the ascending phase as compared to the descending one.

A clear difference between SC23 and 24 as far as it concerns the possible source of HSSWSs is that the number of CHs associated with HSSWSs in SC23 was greater than that of the current one. Contrary to the previous solar cycle, in which the majority of the defined HSSWSs, 66.4%, were produced by coronal holes (Xystouris, Sigala, and Mavromichalaki, 2014), in the current solar cycle the respective percentage reached only a value of 37%.

**Table 5** Yearly number of geomagnetic storms (G), minor (G1), moderate (G2), strong (G3), and severe (G4) during 2009–2016.

| Years        | Total storms (G) | Minor (G1) | Moderate (G2) | Strong (G3) | Severe (G4) |
|--------------|------------------|------------|---------------|-------------|-------------|
| 2009         | 4                | 2          | 2             | 0           | 0           |
| 2010         | 17               | 12         | 4             | 1           | 0           |
| 2011         | 27               | 15         | 8             | 2           | 2           |
| 2012         | 34               | 20         | 12            | 2           | 0           |
| 2013         | 21               | 15         | 5             | 1           | 0           |
| 2014         | 26               | 20         | 5             | 1           | 0           |
| 2015         | 59               | 34         | 18            | 4           | 3           |
| 2016         | 56               | 39         | 14            | 3           | 0           |
| <i>Total</i> | 244              | 157        | 68            | 14          | 5           |

We remark that there are many observed differences between odd and even solar cycles. Even cycles, as SC24, seem to be less active than odd ones (Mavromichalaki and Vassilaki, 1998). As is shown in previous work concerning Solar Cycles 20, 21, and 22 the majority of HSSWSs last around four to six days for even cycles and almost six to eight days for odd ones (Maris and Maris, 2005). Moreover, Gupta and Badruddin (2010) separated the streams that occurred in SC23 into three categories: short-duration high-speed streams (HSSs) with  $t \leq 4$  days, medium-duration HSSs with  $4 \leq t \leq 8$  days, and long-duration HSSs with  $t \geq 8$  days, with percentages of 12%, 46% and 43% out of the total 465 high-speed streams. Moreover, they remarked that HSSs with duration  $t \leq 4$  days are more frequent in the rising phase, while in the declining phase the medium-duration HSSs are fewer and during the maximum and declining phases of SC23 the long-duration HSSs are dominant. These conclusions are consistent with the results of this study since the greatest number of HSSWSs lasted between four–six days (95 of the total 303 HSSWSs that means a percentage of 31%).

### 3.6. HSSWSs and Geomagnetic Storms

When a very efficient exchange of energy between the solar wind and the near-Earth space exists, a great disturbance of Earth's magnetosphere occurs, which is called geomagnetic storm (GS). The time intervals of high-speed solar wind with a southward directed solar wind magnetic field at the dayside of the magnetosphere correspond to the effective conditions for causing GSs. The more intense storms are associated with CMEs, which typically take several days to arrive at Earth, but some of the most intense storms have been observed to start in less than 18 h. Another solar wind disturbance that is favorable to GSs is an HSSWS that plows into the slower solar wind in front of it and creates a corotating interaction region (CIR). These regions are often related to GSs though less intense than CME storms, but they can often deposit more energy in the Earth's magnetosphere over a longer interval (<http://www.swpc.noaa.gov/phenomena/geomagnetic-storms>).

In this work, we have isolated the GSs during the period 2009–2016. We have separated them into four scales, minor (G1), moderate (G2), strong (G3), and severe (G4) following the NOAA classification ([http://www.swpc.noaa.gov/NOAA\\_scales](http://www.swpc.noaa.gov/NOAA_scales)). This categorization is based on the  $K_p$  index values,  $K_p = 5, 6, 7, 8-9$ , respectively. The yearly number of these storms is given in Table 5, while the time distribution of the total number of storms is presented

in the lower panel of Figure 2. It is important to note that the occurrence of storms follows an 11-year distribution with the exception of 2015 and 2016, which, although being in the declining phase of the current cycle, are characterized by a large number of HSSWSs and intense GSs.

The yearly number of the HSSWSs associated with GSs in the four scales separately is given in Table 6. The enhanced number of minor storms associated with HSSWSs is also presented in this table. A separation of the storms associated with HSSWSs originating from CMEs or CHs has also been done and the yearly number of these categories for 2009–2016 is given in the two last columns of Table 6. The time distribution of the four types of geomagnetic storms associated with HSSWSs originating from CMEs or CHs is given in the upper and lower panels of Figure 7, respectively. It is noted that the number of minor geomagnetic storms, G1, in both cases is enhanced during the maximum of the cycle and a great increase is observed in 2015 and 2016 at the declining phase of the cycle. The same behavior is observed with moderate storms, G2, increasing in the case of HSSWSs originating from CMEs. The number of the strong, G3, and severe, G4, storms is lower.

According to Watari (2018) intense GSs associated with coronal holes were also observed under the weak solar wind conditions of Cycle 24. The yearly averaged solar wind speed is also lower in Cycle 24 than in Cycles 22 and 23. Previous studies have shown that only a small number of intense geomagnetic storms ( $Dst < -100$  nT) were caused by high-speed solar wind flows from coronal holes. A complex catalog of high-speed streams and geomagnetic storms during SC24 has been recently published by Muntean, Besliu-Ionescu, and Dobrica (2018). This catalog considers the HSSWSs caused only by coronal holes and their association with geomagnetic storms defined by the  $Dst$  index. The difference between this catalog and the one in this work is based on the determination of the possible sources of the HSSWSs obtained in our case from the interval of two days before the stream and the classification of the geomagnetic storm according to the  $K_p$  index. Additionally, in a recent work by Melkumyan *et al.* (2018) a study of the effects of high-speed solar wind streams originated from coronal holes on cosmic ray events, such as Forbush decreases, is discussed. The authors note that Forbush decreases generated by CMEs are more strongly dependent on the characteristics of interplanetary disturbances compared to those related to coronal holes. This conclusion leads to idea of significant differences in the modulation mechanism between the two types of Forbush decreases.

#### 4. Results and Conclusions

The identification of 303 HSSWSs that occurred during the time period 2009–2016, covering the deep minimum between the previous SC23 and the current SC24 as well as the rising, the maximum, and most of the descending phase of this solar cycle, is presented in this work. Additionally, a comprehensive study of the main properties of the identified HSSWSs in relation to the associated magnetic activity is also given.

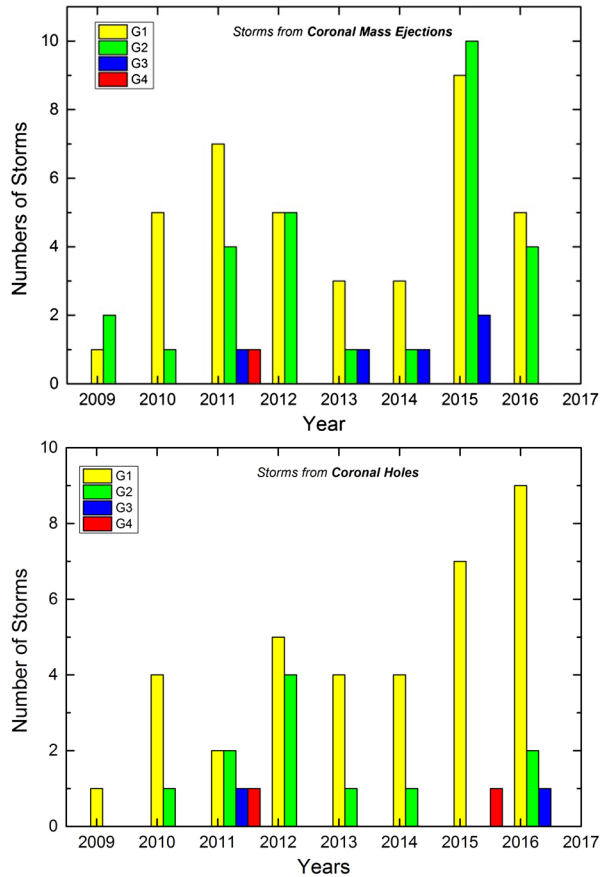
Summarizing the main findings are the following:

- a) The current solar cycle is characterized by a relatively small number of HSSWSs in relation to the previous SC23, while the majority of them originate from CMEs contrary to the previous solar cycle, in which most registered HSSWSs resulted from CHs (Xystouris, Sigala, and Mavromichalaki, 2014).
- b) As is well known, SC24 is characterized by low solar activity and we find that the average duration of the HSSWSs ranges from four to six days. Compared with the previous SC23,

**Table 6** Yearly number of the total (G), minor (G1), moderate (G2), strong (G3) and severe (G4) HSSWS-associated storms and yearly number of geomagnetic storms caused by HSSWSs from CMEs and CHs during 2009–2016.

| Years        | Total HSSWS/storms (G) | Minor (G1) | Moderate (G2) | Strong (G3) | Severe (G4) | HSSWS <sub>CME</sub> /storms | HSSWS <sub>CH</sub> /storms |
|--------------|------------------------|------------|---------------|-------------|-------------|------------------------------|-----------------------------|
| 2009         | 4                      | 2          | 2             | –           | –           | 3                            | 1                           |
| 2010         | 11                     | 9          | 2             | –           | –           | 6                            | 5                           |
| 2011         | 18                     | 9          | 6             | 2           | 1           | 11                           | 7                           |
| 2012         | 19                     | 10         | 9             | –           | –           | 10                           | 9                           |
| 2013         | 10                     | 7          | 3             | –           | –           | 5                            | 5                           |
| 2014         | 10                     | 8          | 2             | –           | –           | 5                            | 5                           |
| 2015         | 29                     | 15         | 10            | 2           | 2           | 21                           | 8                           |
| 2016         | 21                     | 14         | 6             | 1           | –           | 9                            | 12                          |
| <i>Total</i> | 122                    | 74         | 40            | 5           | 3           | 70                           | 52                          |

**Figure 7** Yearly distribution of the four types of geomagnetic storms, G1, G2, G3, and G4, caused by HSSWSs associated with CMEs (*upper panel*) and with CHs (*lower panel*).



we would like to point out that this duration tends to be more or less greater than in the previous one, in which it was found to be from three to five days. On the other hand, the distribution of HSSWSs according to their maximum speed during the different phases of SC24 presents slightly smaller values than in the previous SC23 (Xystouris, Sigala, and Mavromichalaki, 2014). This possibly results from the low activity of the Sun during the current cycle.

- c) As far as it concerns the associated solar structure of HSSWSs we distinguish them into two categories: HSSWSs ejected from active regions of the Sun during CMEs and those originating from a diverging and unipolar field known as a CH. Therefore two classes of interplanetary structures are associated with the two types of the solar magnetic field topology: ICMEs and CIRs (Gosling *et al.*, 1976; Gopalswamy, Yashiro, and Akiyama, 2007; Jian *et al.*, 2006). Both ICMEs and CIRs can drive shocks in the interplanetary space through the interaction between high-speed streams from CMEs and/or from CHs and the surrounding solar wind. Based on our criteria, the majority of HSSWSs are found to originate from CMEs. Despite the fact that the number of CME-generated HSSWSs is quite greater than the one of CH-generated streams throughout the whole SC24, in 2015 an extremely high number of CME-generated HSSWSs has been recorded. This indicates the essential contribution of CME-generated HSSWSs in influencing the geomagnetic activity and creating the geomagnetic disturbances.

- d) According to our findings the majority of all identified HSSWSs of SC24 last four to six days, have a maximum speed between  $500\text{--}599\text{ km s}^{-1}$ , and originate from CMEs.
- e) There is an obvious deviation from the 11-year variation in the declining phase of SC24 specifically during 2015. This year is characterized by a great number of HSSWSs. It is important to note that this year was characterized by long geomagnetic quiet periods with a lot of geomagnetic active breaks, although this year is in the declining phase of the current SC24. As a result a great number of geomagnetic storms from G1 up to G4 scales are found.
- f) During SC24, a 40% of the total identified HSSWSs were followed by geomagnetic storms. Note that the percentage of HSSWSs originating from coronal holes that caused geomagnetic storms is almost the same as the one originating from CMEs. This result indicates the importance of HSSWSs as a driver of geomagnetic activity within the Earth's magnetosphere. Despite the fact that HSSWSs are not ordinarily connected with Dst index values below  $-50\text{ nT}$ , they do produce moderate levels of long duration geomagnetic activity.
- g) The yearly distribution of storm-related HSSWSs for both categories, those originating from coronal holes and those originating from coronal mass ejections, presents the same behavior during the different phases of SC24 with an exception of 2015. During this year a sharp increase in the number of CME-originated HSSWSs reveals this category HSSWSs to be more important in generating storms than the CH-originated ones.

Finally, we would like to mention that in the last years it has been found that the geomagnetic activity in Earth's magnetosphere is in a high measure driven by solar wind streams (Friedel, Reeves, and Obara, 2002). Whereas CMEs can produce geomagnetic storms during the solar maximum, during the declining and minimum phases of solar activity an increase in the occurrence rate of HSSWSs ( $450\text{ km s}^{-1}$ ) originating from coronal holes is also observed (Richardson, Cane, and Cliver, 2002). Despite the fact that HSSWSs are not regularly associated with large geomagnetic disturbances, decreases in the Dst index above  $-50\text{ nT}$ , cause long-lasting moderate geomagnetic activity levels. Conversely, CMEs are more sporadic and cause intense geomagnetic levels lasting only one to two days (Richardson, 2013). So, the energy which enters the magnetosphere during HSSWS events is comparable to or may exceed the one entering from CMEs. Moreover, the HSSWS-driven storms caused more important enhancements in electron flux than CME-driven storms, presenting a high-energy peak flux later in time together with the enhancement of various magnetospheric processes.

**Acknowledgements** We appreciate the contribution of the OMNI Web database of NASA/GSFC providing the necessary data for the definition of the HSSWSs. The websites [http://www.olen.info/solar/coronal\\_holes.html](http://www.olen.info/solar/coronal_holes.html) and [http://cdaw.gsfc.nasa.gov/CME\\_list/](http://cdaw.gsfc.nasa.gov/CME_list/), providing data for the coronal holes and for the coronal mass ejections, respectively, are also acknowledged.

**Conflict of interest** The authors indicate that they have no conflict of interest.

## References

- Aslam, O.P.M., Badruddin: 2017, Study of the geoeffectiveness and galactic cosmic-ray response of VarSITI-ISEST campaign events in Solar Cycle 24. *Solar Phys.* **292**, 17. DOI.
- Badruddin, Falak, Z.: 2016, Study of the geo-effectiveness of coronal mass ejections, corotating interaction regions and their associated structures observed during Solar Cycle 23. *Astrophys. Space Sci.* **361**, 253. DOI.
- Badruddin, Kumar, A.: 2015, Study of the Forbush decreases, geomagnetic storms, and ground-level enhancements in selected intervals and their space weather implications. *Solar Phys.* **290**, 127. DOI.



- Badruddin, Singh, Y.P.: 2009, Geoeffectiveness of magnetic cloud, shock/sheath, interaction region, high-speed stream and their combined occurrence. *Planet. Space Sci.* **57**, 318. DOI.
- Bame, S.J., Asbridge, J.R., Feldman, W.C., Gosling, J.T.: 1976, Solar cycle evolution of high-speed solar wind streams. *Astrophys. J.* **207**, 977.
- Belov, A., Baisultanova, L., Eroshenko, E., Mavromichalaki, H., Yanke, V., Pchelkin, V., Plainaki, C., Mariatos, G.: 2005, Magnetospheric effects in cosmic rays during the unique magnetic storm on November 2003. *J. Geophys. Res.* **110**, A09S20. DOI.
- Bothmer, V., Zhukov, A.N.: 2007, The Sun as the prime source of space weather. In: Daglis, J. (ed.) *Space Weather – Physics and Effects*. DOI. Chapter 3.
- Cane, H.V.: 2000, Coronal mass ejections and Forbush decreases. *Space Sci. Rev.* **93**, 55. DOI.
- Crooker, N.U., Shodhah, S., Gosling, J.T., Simmerer, J., Steinberg, J.T., Kahler, S.W.: 2000, Density extremes in the solar wind. *Geophys. Res. Lett.* **27**, 3769. DOI.
- de Toma, G.: 2011, Evolution of coronal holes and implications for high-speed solar wind during the minimum between Cycles 23 and 24. *Solar Phys.* **274**, 19. DOI.
- Eroshenko, E., Belov, A., Mavromichalaki, H., Mariatos, G., Oleneva, V., Plainaki, C., Yanke, V.: 2004, Cosmic ray variations during the two great bursts of solar activity in the 23rd solar cycle. *Solar Phys.* **224**, 345. DOI.
- Friedel, R.H.W., Reeves, G.D., Obara, T.: 2002, Relativistic electron dynamics in the 612 inner magnetosphere – a review. *J. Atmos. Solar-Terr. Phys.* **64**, 265.
- Gopalswamy, N., Yashiro, S., Akiyama, S.: 2007, Geoeffectiveness of halo coronal mass ejections. *J. Geophys. Res. Space Phys.* **112**, A06112. DOI.
- Gopalswamy, N., Akiyama, S., Yashiro, S., Xie, H., Mäkelä, P., Michalek, G.: 2014, Anomalous expansion of coronal mass ejections during Solar Cycle 24 and its space weather implications. *Geophys. Res. Lett.* **41**, 2673. DOI.
- Gosling, J.T., Asbridge, J.R., Bame, S.J., Feldman, W.C.: 1976, Solar wind speed variations: 1962–1974. *J. Geophys. Res.* **81**, 5061. DOI.
- Gupta, V., Badruddin: 2009, Interplanetary structures and solar wind behavior during major geomagnetic perturbations. *J. Atmos. Solar-Terr. Phys.* **71**, 885.
- Gupta, V., Badruddin: 2010, High-speed solar wind streams during 1996–2007: sources, statistical distribution, and plasma/field properties. *Solar Phys.* **264**, 165. DOI.
- Jian, L., Russell, C.T., Luhmann, J.G., Skoug, R.M.: 2006, Properties of interplanetary coronal mass ejections at one AU during 1995–2004. *Solar Phys.* **239**, 393. DOI.
- Kane, R.P.: 2007, Solar terrestrial effects of two distinct types. *Adv. Space Res.* **39**, 1890. DOI.
- Kudela, K., Brenkus, R.: 2004, Cosmic ray decreases and geomagnetic activity: list of events 1982–2002. *J. Atmos. Solar-Terr. Phys.* **66**, 1121. DOI.
- Kumar, A., Badruddin: 2014, Cosmic ray modulation due to high speed solar wind streams of different sources, speed and duration. *Solar Phys.* **289**, 4267. DOI.
- Lakhina, G., Tsurutani, B.T.: 2016, Geomagnetic storms: historical perspective to modern view. *Geosci. Lett.* **3**, 5. DOI.
- Lindblad, A., Lundstedt, H.: 1981, A catalogue of high-speed plasma streams in the solar wind. *Solar Phys.* **74**, 197. DOI.
- Lindblad, B.A., Lundstedt, H.: 1983, A catalogue of high speed plasma streams in 1975–1978. *Solar Phys.* **88**, 377. DOI.
- Lindblad, B.A., Lundstedt, H., Larsson, B.: 1989, A third catalogue of high-speed plasma streams in the solar wind – data for 1978–1982. *Solar Phys.* **120**, 145. DOI.
- Maris, O., Maris, G.: 2005, Specific features of the high-speed plasma stream cycles. *Adv. Space Res.* **35**, 2129.
- Mavromichalaki, H., Vassilaki, A.: 1998, Fast plasma streams recorded near the Earth during 1985–1996. *Solar Phys.* **183**, 181. DOI.
- Mavromichalaki, H., Vassilaki, A., Marmatsouri, E.: 1988, A catalogue of high-speed solar wind streams – further evidence of their relationship to  $A_p$ -index. *Solar Phys.* **115**, 345. DOI.
- Melkumyan, A.A., Belov, A.V., Abunina, M.A., Abunin, A.A., Eroshenko, E.A., Oleneva, V.A., Yanke, V.G.: 2018, Main properties of Forbush effects related to high-speed streams from coronal holes. *Geomagn. Aeron.* **58**, 154. DOI.
- Muntean, G.M., Besliu-Ionescu, D., Dobrica, V.: 2018, Complex catalogue of high speed streams and geomagnetic storms during solar cycle 24 (2009–2016). *VarSITI Newsletter* **17**, 5.
- Paouris, E., Gerontidou, M., Mavromichalaki, H.: 2016, The geomagnetic storms of 2015: statistical analysis and forecasting results. *Geophys. Res. Abstr.* **18**, EGU2016-11753.
- Paouris, E., Mavromichalaki, H.: 2017, Interplanetary coronal mass ejections resulting from Earth-directed CMEs using SOHO and ACE combined data during Solar Cycle 23. *Solar Phys.* **292**, 30. DOI.

- Papaioannou, A., Belov, A., Mavromichalaki, H., Eroshenko, E., Oleneva, V.: 2009a, The unusual cosmic ray variations in July 2005 resulted from western and behind the limb solar activity. *Adv. Space Res.* **43**, 582. [DOI](#).
- Papaioannou, A., Mavromichalaki, H., Eroshenko, E., Belov, A., Oleneva, V.: 2009b, The burst of solar and geomagnetic activity in August–September 2005. *Ann. Geophys.* **27**, 1019.
- Parker, E.: 1959, Extension of the solar corona into interplanetary. *J. Geophys. Res.* **64**, 1675.
- Richardson, I.G.: 2013, Geomagnetic activity during the rising phase of solar cycle. *J. Space Weather Space Clim.* **3**, A08. [DOI](#).
- Richardson, I.G., Cane, H.V., Cliver, E.W.: 2002, Sources of geomagnetic activity during nearly three solar cycles (1972–2000). *J. Geophys. Res.* **107**, SSH 8-1. [DOI](#).
- Sabbah, I.: 2000, The role of interplanetary magnetic field and solar wind in modulating both galactic cosmic rays and geomagnetic activity. *Geophys. Res. Lett.* **27**, 1823. [DOI](#).
- Wang, Y.M.: 2010, On the relative constancy of the solar wind mass flux at 1 AU. *Astrophys. J. Lett.* **715**(2), 121. [DOI](#).
- Watari, S.: 2018, Intense geomagnetic storms associated with coronal holes under the weak solar-wind conditions of cycle 24. *Solar Phys.* **293**, 23. [DOI](#).
- Xystouris, G., Sigala, E., Mavromichalaki, H.: 2014, A complete catalogue of high-speed solar wind streams during solar cycle 23. *Solar Phys.* **289**, 995. [DOI](#).
- Yermolaev, Y.I., Ladkina, I.G., Nikolaeva, N.S., Yermolaev, M.Y.: 2014, Influence of the interplanetary driver type on the durations of the main and recovery phases of magnetic storms. *J. Geophys. Res.* **119**, 8126. [DOI](#).